Diatom-based paleolimnology of Lake Pavin over the past 7000 years

Karen K Serieyssol, Aude Beauger, Yannick Miras, Léo Chassiot, Victor Arricau, Emmanuel Chapron

J Paleolimnol
https://doi.org/10.1007/s10933-024-00330-2

ORIGINAL PAPER

Diatom-based paleolimnology of Lake Pavin over the past 7000 years

Karen K. Serieyssol · Aude Beauger · Yannick Miras · Léo Chassiot · Victor Arricau · Emmanuel Chapron

Received: 17 May 2024 / Accepted: 10 June 2024

Abstract Lake Pavin, a maar lake was formed approximately 7000 years ago by a phreatomagmatic explosion, leaving a deep central crater with shallow steep side slopes. PAV12 core, collected from the center of the lake, displayed two diatomite layers, separated by a 4-m thick unit of reworked sediments. Diatom diversity and zonation analyses registered six zones documenting the lake evolution. *Asterionella formosa, Pantocsekiella ocellata* and *Discostella pseudostelligera* (including f. *diminuta*) along with fragilariod taxa composed the basal unit (L-1, ~ 6900 to 6570 cal a BP). With increased mineralization of the lake waters, *Stephanodiscus* taxa became the major species (L-2, 6190–3800 cal a BP). A transition zone was noted between Zone L-2 and L-3 (3950–3700 BP) and related to a major change in diatom composition. *Asterionella formosa* and *Nitzschia paleacea* dominated Zone L-3 (3760–1470 cal a BP) with a large decrease in *Stephanodiscus* taxa. This major change has been related to soil erosion and the possible development of meromixis. *Stephanodiscus parvus* and *Asterionella formosa* dominated the upper diatomite zone L-4 (640–400 cal a BP) while zone L-5 (290–160 cal a BP) is dominated by *Aulacoseira subarctica* (including f. *recta*) and may be caused by the Little Ice Age. Zone L-6 (subrecent) saw a return to similar conditions as in zone L-4. The gradual opening of the diversified forest and appearance of regional agriculture appears to be related to the development of meromixis. Changes in the upper diatomite zone are related to agricultural activity, changes in incomplete overturn and climate. This study examines relationships between diatom changes and pollen and geochemical changes observed within the lake.

Keywords Siliceous component · Pollen · Environmental changes · Chemical changes

K. K. Serieyssol (✉)
Laboratoire EVS-ISTHME, UMR 5600 – CNRS, Université de Lyon, 6 rue Basse des Rives, 42023 Saint-Etienne Cedex 2, France
e-mail: karenkserieyssol@aol.com

A. Beauger
CNRS, GEOLAB, Université Clermont Auvergne, 63000 Clermont-Ferrand, France

Y. Miras
CNRS, Histoire Naturelle de l'Homme Préhistorique (HNHP) UMR 7194, Muséum National d'Histoire Naturelle, Institut de Paléontologie Humaine, 1 rue René Panhard, 75013 Paris, France

L. Chassiot · E. Chapron
Département de Géographie, Pavillon Abitibi-Price, Université Laval, 2405 rue de la Terrasse, Quebec, QC G1V0A6, Canada

L. Chassiot · V. Arricau · E. Chapron
Géographie de l'Environnement (GEODE) UMR 5602 CNRS, Université Toulouse 2 Jean Jaurès, Allée A. Machado, 31058 Toulouse Cedex, France

Published online: 24 July 2024

Introduction

Lake classification is based on the seasonal thermal conditions that determine stratification and mixing processes. These conditions are affected by changes in lake morphometry such as the depth or the surface area that are related to the origin of the lake. Moreover, the drainage-basin morphometry and the dissolved and suspended solids in the waters also affect these conditions (Hall and Northcote 2012). Among the different types of lakes are maar-crater lakes that are formed by an explosive volcanic event creating a funnel-shaped basin, with a small deep circular center and shallow steep slope surrounding it. The created watershed is usually very small, often the size of the crater. However, some fracturing of the ground around the puncture hole, or former punctured lava-flow deposits may allow local water to infiltrate into the maar lake (Busigny et al. 2016), and the hydrological catchment area can be larger than the topographic catchment area (Chapron et al. 2021). These lakes are ideal for researchers studying local climate change as only local precipitation will affect the lake environment through ground water infiltration from a geographically small local water basin and direct inflow from the crater slopes. Diatoms are generally well-preserved in maar-crater lakes where silica-rich waters are not a limiting factor in diatom production, thereby creating well-preserved diatomite (Battarbee et al. 2001). The environmental studies of many maar lakes from all over the world have used diatoms and/or pollen. Indeed, diatoms provide local information based on their ecological preferences, particularly chemical and water-depth changes observed in the lake while pollen provide both local and regional information, as they depend mostly on aerial deposition. By combining the pollen and diatom analyses, local changes may be separated from regional effects, as wind-blown diatoms are rarely found in sediment traps because the water-surface tension protects lacustrine diatoms from becoming windblown (Harper and McKay 2010).

Diatoms have been studied from a series of maars located in the French Massif Central (Gasse 1969; Pailles 1989; Kuehlthau-Serieyssol 1993; Rioual 2000, 2002; Stebich et al. 2005; Pastre et al. 2007; Rioual et al. 2007) with reconstructions spanning from the Upper Miocene, Middle Pleistocene to present. Among the maar lakes situated in the Massif Central, Lake Pavin (Fig. 1) is one of the youngest formed maar craters (7000 years ago). Its topographic catchment area includes the crater rim and the southern part of the Puy de Montchal volcano, cut by the Pavin phreatomagmatic explosion (Chapron et al. 2012; Chassiot et al. 2016b; Thouret et al. 2021). It is a meromictic lake that has two layers of water that typically do not mix. The lake rarely undergoes complete overturn while in ordinary, holomictic lakes overturn occurs at least once a year: the surface layers and deep waters are mixed together. A meromictic lake occurs when "salinity or turbidity gradients set up concentration profiles with enough density difference to bring about stability of their lower layers" (Hall and Northcote 2012).

Lake Pavin has a long and extensive scientific history starting with the Chevalier's Expedition in 1770, but with the discovery of the lake's meromixis (Olivier 1952; Pelletier 1963, 1968), Lake Pavin acquired a status as an international field laboratory (Meybeck 2016). The first person to look at diatoms from Lake Pavin was Manquin (1954). He studied material dredged from the deepest section of the lake and determined 130 species. Later, Gasse (1969) and then Stebich et al. (2005) both studied short cores covering only the last 700 years. Over the last decades, scientific investigations of the water column highlighted several specific biogeochemical aspects of the Pavin hydrosystem (Sime-Ngando et al. 2016). Sedimentary archives and geophysical mapping allowed reconstruction of Holocene paleoenvironments, water level changes (Stebich et al. 2005; Chassiot et al. 2018) and the assessment of natural hazards (Chapron et al. 2010; Chassiot et al. 2016a, 2016b, 2018).

Moreover, recent studies have focused on the fluctuations of Lake Pavin's elevation in relation with erosional processes of the crater and regional paleoearthquakes (Miallier 2020; Thouret et al. 2021; Chapron et al. 2021). Miallier (2020) and Thouret et al. (2021) both noted two lake terraces within the crater: the highest one (1215 m a.s.l.) at + 18 m above current lake level and dated prior to the 5–7 century CE, while a second stillstand occurred + 4.35 m (1201 m a.s.l.) above present lake level (1997 m a.s.l.) and finally the present day's lake level which was stabilized by the development of a dike between 1859 and 1860 (Miallier 2020; Thouret et al. 2021). There was a gradual downcutting of the maar rim between

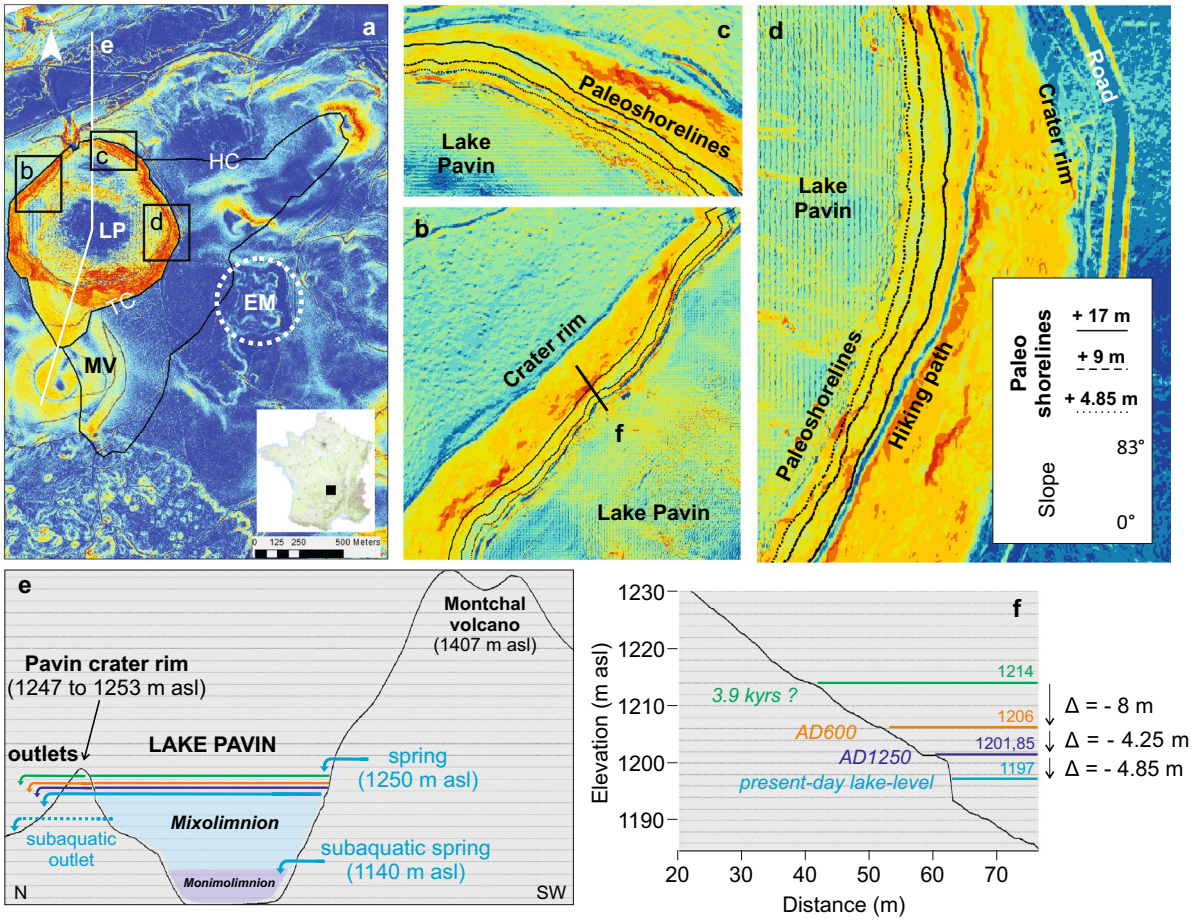

Fig. 1 **a** Slope map of the Montchal-Pavin geosystem combining terrestrial LiDAR and multibeam swath bathymetry (Chapron et al. 2010), with topographic (TC) and hydrographic (HC) catchments. LP: Lake Pavin; MV: Montchal Volcano; EM: Estavidoux Maar. The inlet indicates the location in the Massif Central, France. **b**, **c** and **d** zoom on the crater slope illustrating paleoshorelines. **e** Elevation profile across the Montchal-Pavin geosystem (see a for the location) showing former lake levels (colored arrows), springs and outlet positions (light blue arrows). **f** Elevation profile showing paleoshoreline altitudes and estimated ages (see b for the location). Colors used are the same as for e)

the highest terrace and the second one and more rapid erosion between the second stillstand to the present lake level. The increase in downcutting could have resulted from heavy rainstorms (Throuret et al. 2021). However, the LiDAR cover for the crater allowed Arricau et al. (2020) to identify a series of terraces representing former lake levels at 1214, 1206, and 1201.85 m, respectively, which reflects a total drop of 17 m to reach the modern elevation at 1197 m a.s.l. (Fig. 1). Nevertheless, the 1206 terrace is poorly represented.

In order to get a better understanding of the complete history of Lake Pavin, the longest continuous core so far taken from Lake Pavin was studied. Until now, only preliminary diatom results have been presented by Chassiot et al. (2016a). With core PAV12, our main objectives are (1) to reconstruct diatom communities from PAV12 core over 7000 years; (2) to give a more complete idea of the changes observed over the whole lake's history by coupling diatom results with pollen and geochemical data, and (3) possibly determine when meromictic conditions developed within the lake. These information would aid in a better understanding of mountain environments and past agro-pastoral activities and human occupation in the region. As Lake Pavin is an important tourist site,

this study can aid in the development of management strategies for the lake and the region.

Material and methods

In 2012, a 14-m long core (PAV12) was taken from the central part of the deep maar (N 45°29′45″, E 2°53″18″) that formed approximately 7000 years ago (Leyrit et al. 2016; Juvigné and Miallier 2016) by a phreatomagmatic explosion (Sime-Ngando et al. 2016). PAV12 core sections were split for visual description and non-destructive analyses (Chassiot et al. 2016a). Multi-proxy analyses of organic and minerogenic fractions, including pollen and non-pollen palynomorph assemblages, were then performed on the upper and lower diatomite units to infer terrigenous and autogenous signals over the last 7000 years (Chassiot et al. 2018). The maar is situated in the Mont Dore massif of the French Massif Central (Fig. 1) at an elevation of 1197 m a.s.l. (Chassiot et al. 2018) (Fig. 1a). It has a diameter of about 750 m with a surface area of 0.44 km^2. For more detailed lacustrine geomorphology and sedimentology information refer to Chapron et al. (2010, 2012, 2016) and Chassiot et al. (2016a, 2016b). The rim of the crater is composed mainly of basaltic fragments and trachy-andesitic pumices and covered with a forest composed of beech (*Fagus sylvatica*) and fir (*Abies alba*) and some planted areas composed of spruce (*Picea abies*) (Chassiot et al. 2018). The meteorological station at Besse-en-Chandesse, located 5 km from the lake, recorded a mean temperature near zero degrees in the winter (causing partial or complete freezing) and annual precipitation between 1600 and 1700 mm a^{-1} (Stebich et al. 2005).

The lake topographic catchment area (0.36 km^2) includes the crater rim and the northern part of the Puy de Montchal stratovolcano. Different springs are identified on the southern slopes of the lake (Jezequel et al. 2011; Chapron et al. 2016) and there are also subaquatic springs located at ca. 55 m water depth (Bonhomme et al. 2016; Chassiot et al. 2018). A minimum hydrographic drainage basin for Lake Pavin is at least ca. 4.21 km^2 (Fig. 1A), including a small marsh land at the location of the former Estivadoux Maar (Arricau 2020). LiDAR cover for the crater allowed Arricau (2020) to identify a series of terraces.

Lake Pavin is meromictic; the deep water monimolimnion is the lower dense layer of the lake that does not mix with the waters above (mixolimnion). It is permanently anoxic with iron-rich waters and high concentrations of biogenic and mantle-derived gases. The boundary between the monimolimnion and the mixolimnion is located between 53 and 56 m water depth, caused by underwater springs with low oxygen and saline contents (Bonhomme et al. 2016) (Fig. 1e). Areas of spring water rise up through the water column suggesting intermittent discharges. The partial seasonal overturn (i.e., of the mixolimnion) is linked to winter meteorological conditions and spring inflows (Bonhomme et al. 2016). According to Rioual (2002), the actual lake is rich in silica (14.9 mg L^{-1}), total phosphorus (TP) of 10 µg L^{-1}, NO_3–N (40 µg L^{-1}) and has a pH of 6.5. The deep layers are stabilized by heat and increasing dissolved chemical concentration and only over a long period of time could react with the mixolimnion (Bonhomme et al 2016).

In core PAV12, two diatomite layers (upper and lower diatomite units) are observed separated by a mass wasting deposit (MWD) caused by regional earthquakes at ca. 600 and ca. 1300 CE (Chapron et al. 2010, 2021; Chassiot et al. 2016a, 2016b). It was distinguished by a highly disrupted diatomite lamina, high spectrophotometric and organic content variability, and a reversal of age dating (Chassiot et al. 2016b). The stratigraphy of PAV12 can be summarized as follow: (1) an upper diatomite unit (0–228 cm, 14 samples studied), a MWD (228–628 cm), a lower diatomite unit (628–1045 cm, 67 samples studied), and a basal unit (1045–1400 cm, 7 samples studied) "made of laminated volcanoclastic materials interbedded with turbidites" (Chassiot et al. 2018).

In PAV12 core, diatom and pollen samples were taken from the same levels (Chassiot et al. 2018). Since high-resolution pollen and lesser-resolution diatom study already exists for the upper diatomite unit (Stebich et al. 2005), efforts were focused on the lower unit of PAV12 found in the deep basin. Seventy-seven samples coming from the lower diatomite unit were studied with a sampling resolution of approximately every 5 cm. Consequently, the sampling resolution was larger with only 14 samples for the upper diatomite unit (ca. every 8–20 cm). However, between 781 and 828 cm, 47 cm or 8 samples are missing.

Diatoms were cleaned using the method described in Serieyssol et al. (2010) using 30% H_2O_2, rinsed three times and then mounted in Naphrax®. Identification and counts were made using a Leica microscope DM2700M or a Zeiss Axioskop 2 at 1000× magnification. Diatoms were identified using Krammer and Lange-Bertalot (1997a, b, 2000, 2004), Krammer (2002, 2003), Houk et al. (2010, 2014) and Lange-Bertalot (2001). The names were updated using Algaebase (www.algaebase.org). Over 400 valves were counted using two different slides. Data analysis was based on species occurring in greater abundance than 1% and in more than one sample to minimize the influence of rare taxa.

Detailed information on pollen-sample preparations, identification references and data-percentage calculations were given in Chassiot et al (2018): an average of 500 pollen grains per sample from terrestrial plants were counted. Redundancy Analysis (RDA) was performed using PC-ORD 7.07 (McCune and Mefford 2018). RDA explores the relationship between two different matrices and the following options were used: centered but not standardized, scaling 1—distance bipot, and linear combination of species (fitted site scores) with randomization test (999). Diatom, assemblage groups were determined with Psimpoll 4.26 (Bennet 2002) using CONISS, zonation with constrained cluster analysis by sum-of-squares. The ecological categories are largely based on Van Dam et al. (1994) and Denys (1991).

Diatom data were compared to Si/Ti, Fe and total organic carbon (TOC) data. The geochemical data used in this article come from previously published articles (Chassiot et al. 2016b, 2018), where they discuss how the samples were treated. Eleven leaf samples were used in dating the PAV12 core. Two for the upper diatomite unit, one in the MDW, and eight for the lower diatomite unit. One leaf sample was rejected for large discrepancy of time in relationship to the others. The radiocarbon dating method was described in Chassiot et al. (2016a).

Results

Diatom stratigraphy

Over 187 different diatom species were observed, but only 27 species were found to be present with an abundance of at least 1% and in more than one sample. *Discostella pseudostelligera* was combined with f. *diminuta*, and *Staurosira construens* was combined with *Staurosira binodis*. Table 1 lists the 22 species used in the analyses and their percentage variation in each zone and their life form based on Denys (1991).

Six zones (Fig. 2) were determined based on the repartition of the major species that occurred in equal or greater abundance than 1% in one or more samples. Three zones in the lower diatomite unit and three in the upper diatomite unit (Fig. 2). Zone L-1 (1260–1021 cm; ca. 6900–6570 cal a BP) is dominated by *A. formosa*, *C. ocellata*, and *D. pseudostelligera* plus f. *diminuta* with lesser amounts of fragilarioid species (*Pseudostaurosira brevistriata, Staurosirella pinnata* complex and *Staurosira* and *Fragilaria* taxa). Zone L-2a (1015–988 cm; ca. 6490–6130 cal a BP) is dominated by the *Stephanodiscus* taxa: *S. alpinus*, *S. minutulus* and *S. parvus*. The total percentage of *Stephanodiscus* taxa is greater than 80%. However, in Zone L-2b (983–977 cm; ca. 6070–5970 cal a BP), the three *Stephanodiscus* taxa decrease and *Aulacoseira subarctica* appears and varies between 35 and 63%. With zone L-2c (973–838 cm; ca. 5910–3800 cal a BP) the three dominant species found in zone L-2a return.

A major compositional change occurred between zone L-2 and L-3. In zone L-3 (835–628 cm; ca. 3760–1470 cal a BP), *A. formosa* becomes dominant (up to 83%) along with *N. paleacea* (5–61%), and the *Stephanodiscus* species decrease and in certain levels disappear (Table 1). A large, reworked zone of sediment separates the lower diatomite unit from the upper diatomite unit. Three upper diatomite zones were previously investigated by Gasse (1969) and Stebich et al. (2005). Zone L-4 (203–153 cm; ca. 650–400 cal a BP) was determined by large amounts of *Asterionella formosa* and *S. parvus*. *Pseudostaurosira brevistriata* is common. *Aulacoseira subarctica* and f. *recta* become very abundant in zone L-5 (125–78 cm; ca. 290–160 cal a BP) with smaller amounts of *Staurosira construens* and *Staurosirella lapponica* along with decreases in *A. formosa* and *S. parvus*. In zone L-6 (62–1 cm; sub-recent period), the abundant species were *A. formosa* and *S. parvus* again, along with low percentages of *Staurosirella pinnata* complex.

Redundancy analysis

From the 187 species identified, 22 diatom species (> 1% in more than one sample) were retained for the

Table 1 The list of 22 species used in determining the six observed diatom zones in core PAV12

Species / Diatom zones	Upper diatomite			Lower diatomite			Life form
	L-6	L-5	L-4	L-3	L-2	L-1	
Asterionella formosa Hassel	10–49%	3–13%	24–51%	20–83%	0.2–21%	2–45%	eu
Aulacoseira crenulata (Ehr.) Thwaites	0–2%	0–1%	0–1%	0–1%	0%	0–1%	eu
Aulacoseira subarctica (O.F. Müller) E.Y. Haworth	1–9%	5–27%	0–2%	0–8%	0–29%	0–2%	eu
Aulacoseira subarctica f. *recta* O. Müller Krammer	0–15%	26–67%	0%	0–2%	0%	0–0.7%	eu
Stephanodiscus alpinus Hustedt in Huber-Pestalozzi	0–0.2%	0%	0–0.2%	0–2%	1–38%	0–0.2%	eu
Stephanodiscus minutulus (Kützing) Cleve & Möller	0.5–11%	0.7–20%	0.4–10%	0–17%	2–54%	0–19	eu
Stephanodiscus parvus Stoermer & Håkansson	22–62%	2–40%	9–65%	0–10%	1–37%	0.3–48%	eu
Pantocsekiella ocellata (Pantocsek) A. Cleve	0%	0–0.2%	0%	0.2–0.5%	0–0.2%	7–44%	tych
Discostella pseudostelligera (Hustedt) Houk & Klee	0–6%	0.02–3%	0.4–15%	0–15%	0–8%	0.3–33%	tych
Discostella pseudostelligera fo. *diminuta*							tych
Fragilaria gracilis Østrup	0%	0–0.2%	0.06%	0–3%	0–15%	0–0.2%	tych
Staurosira construens Ehr	0–2%	0–2%	0–1%	0%	0%	0–0.2%	tych
Staurosira binodis (Ehr.) P.B. Hamilton							tych
Staurosirella lapponica (Grunow) D.M. Williams & Round	0–0.2%	2–4%	0%	0–0.2%	0%	0%	tych
Fragilaria capucina var. *rumpens* (Kützing) Lange-Bertalot	0–0.7%	0–1%	0–0.7%	0%	0%	0%	tych
Fragilaria capucina var. *vaucheriae* (Kützing) Lange-Bertalot	0–0.4%	0%	0%	0–2%	0–2%	0–0.2%	tych
Staurosira venter (Ehrenberg) Cleve & Möller	0–5%	0%	0–0.3%	0–4%	0–2%	0.4–6%	tych
Gomphonema clavatum Ehr.,	0%	0%	0–1%	0–1%	0–1%	0–0.2%	b–e
Nitzschia paleacea (Grunow) Grunow	0–2%	0–0.7%	0–2%	5–61%	1–39%	0%	b–e
Pseudostaurosira brevistriata (Grunow) D.M. Williams & Round	2–4%	1–3%	4–6%	0–2%	0–0.2%	0–4%	b–e
Staurosirella pinnata (Ehr.) D.M.Williams & Round complex	0.4–1%	0.5–1%	0.2–1$	0–5%	0–1%	0.2–2%	b–e
Ulnaria ulna (Nitzsch) Compère complex	0–1%	0–1%	0–0.07%	0%	0–0.3%	0.2–6%	b–e
Eolimna minima (Grunow) Lange-Bertalot	0–1%	0%	0–2%	0–1%	0–2%	0–0.4%	und
Fragilaria nanana Lange-Bertalot	0%	0–0.5%	0%	0–5%	0–5%	0–2%	und

The taxa were found in percentages equal to or greater than 1% in at least one sample. The percentage range for each species is given for each zone. The characteristic life form for each species is based on Denys (1991). Euplanktonic = eu, tychoplanktonic = tych, benthic–epontic = b-e, undetermined = und

statistical analyses, while 17 pollen variables were used (Fig. 3). Riparian woodland, coniferous woodland, mountain woodland, diversified oak woodland, hazel and other trees represented the forest communities. Anthropogenic factors were arboriculture, grassland, heath, agriculture, hemp, heliophilous herbaceous taxa, tall grass, apophyte (a plant which colonizes areas modified by man), tall grass, spores, riparian plant taxa and ruderals. Two groups were combined (a) nitrophilous and ruderal indicators and (b) ruderal and tramping indicators, as ruderals are the plants which colonize disturbed lands. RDA explained 26.9% of the variance for the first three axes (17.4% the first axis, 9.5% the second axis, with $p = 0.0070$ based on 999 randomizations). RDA axis 1–2 (Fig. 3) found that the majority of the lower diatomite samples (zones L-2 and L-3) were positioned in the lower quadrants while the basal unit (zone L-1) and the upper diatomite units (zones L-4, 5 and 6) were situated in the upper quadrants. *Stephanodicus alpinus* (SA) and *S. minutulus* (SM) determined the lower right quadrant while the lower left quadrant is defined by *Nitzschia paleacea* (NPAE) and *Asterionella formosa* (AF). The upper quadrants were

determined by *Stephanodicus parvus* (SP), *Aulacoseira subarctica* (ASU) plus f. *recta* (ASR) and *Pantocsekiella ocellata* (PC). For the pollen, the right half quadrants were determined by diversified forest (*Quercus, Tilia, Ulmus, Acer*) and hazel bushes, while the upper right half is influenced by coniferous woodland (*Pinus, Juniperus*). The lower left quadrant is determined by mountain forests (*Fagus, Abies*) while upper left quadrant corresponds to numerous agricultural indicators: hemp, riparian (*Alnus, Salix, Fraximus, Populus*) and hygrophytes, agriculture, arboriculture (*Cerealis*-type, *Secale*-type, *Fagopyrum*), arable weed, spores, grasslands (Poaceae), heliophilous herbaceous taxa, heath, apophyte, other herbaceous trees, and ruderals.

Figure 3 shows that most of the basal diatom unit L-1 (green triangles) is situated between the conifer forest and diversified woodland and hazel bushes. This most likely represents a period right after the explosion crater formed and vegetation is regenerating on the land. Two samples (1045 and 1033, the lowest samples in basal unit) are associated with mountain woodland. In diatom zone L-2 (green triangles), there is a gradual shift in the forest composition from diversified forest with hazel towards a mountain forest of *Fagus* and *Abies.* The lowest samples are situated to the far right and the younger samples towards the left. Diatom zone L-3 (brown triangles) is clearly affected by the mountain forest with the development of agriculture and by the influence of ruderal-tramping within the forest. A large mass-wasting deposit separates diatom zone L-3 from L-4. The majority of the samples in the upper diatomite are situated in the upper left half of the RDA. There is a clear shift from the mountain forests to an agricultural influenced landscape in upper diatomite zones. Zones L-4 and L-6 (red triangles) are more strongly influenced by anthropogenic activities than zone L-5. Diatom zone L-5 (red triangles) show an increase in coniferous forests in the area.

Discussion

The lower right quadrant (Fig. 3) is mainly influenced by higher trophic levels and pH. *Stephanodiscus alpinus* and *S. minutulus* dominate samples in the lower right quadrant, *Stephanodiscus alpinus* is widespread in eutrophic waters (Hickel & Håkansson 1993) while *S. minutulus* is considered a hypereutrophic species (Van Dam et al. 1994). Both are considered alkalibiontic (pH = 8.07, Juggins 2001). The lower right quadrant represents lower trophic status with a combination of *N. paleacea* (hypereutrophic) and *A. formosa* (meso-eutrophic) and lower pH preference, both are considered alkaliphilous (Van Dam et al. 1994). Axis 1 represents a pH and trophic gradient with the right side having higher pH values and poorer water quality but with higher biological productivity in the lake.

The upper quadrants (Fig. 3) are associated with *S. parvus*, *P. ocellata,* and *A. subarctica* along *A. subarctica* f. *recta. Aulacoseira subarctica* and *P. ocellata* tolerate very small amount of nitrogen (Van Dam et al. 1994) and prefer continuously oxygen-saturated waters (Van Dam et al. 1994). The lower half quadrant is associated with N-heterotrophic taxa with higher nitrogen demands (*Nitzschia paleacea*—obligately N-heterotrophic, elevated concentrations; *Stephanodiscus minutulus*—periodically elevated concentrations) along with *Asterionella formosa,* a N-autotrophic species that tolerates elevated concentrations (Van Dam et al. 1994). Also, these species occur in waters with lower oxygen content (Van Dam et al. 1994), that varies from relatively high (> 75%, *A. formosa*) to low (> 30%, *S. minutulus*). Axis 2 represents nitrogen and oxygen content, lowest nitrogen content and highest oxygen content in the upper half, while the lower half had higher nitrogen concentration but less oxygen.

Diatom stratigraphy and coupling with pollen and geochemical observations

The basal unit zone L-1 (1260–1021 cm; ca. 6900–6570 cal a BP) marks the formation of the lake and was identified as the basal minerogenic units (Chassiot et al. 2016a) and described as finely laminated volcano clastic sediments thick turbidite beds and massive units intercalated within. Zone L-1 represents the filling-up phase of the crater. At the basis of the zone, brackish-freshwater taxa, typical of mineral springs, are present (*Crenotia thermalis*, *Fragilaria famelica* and *Navicula cincta*) (Beauger et al. 2020), revealing the environment before the development of the lake. This is followed by an increase in planktonic species (*A. formosa*, *Pantocsekiella ocellata*). These taxa belong either to the circumneutral

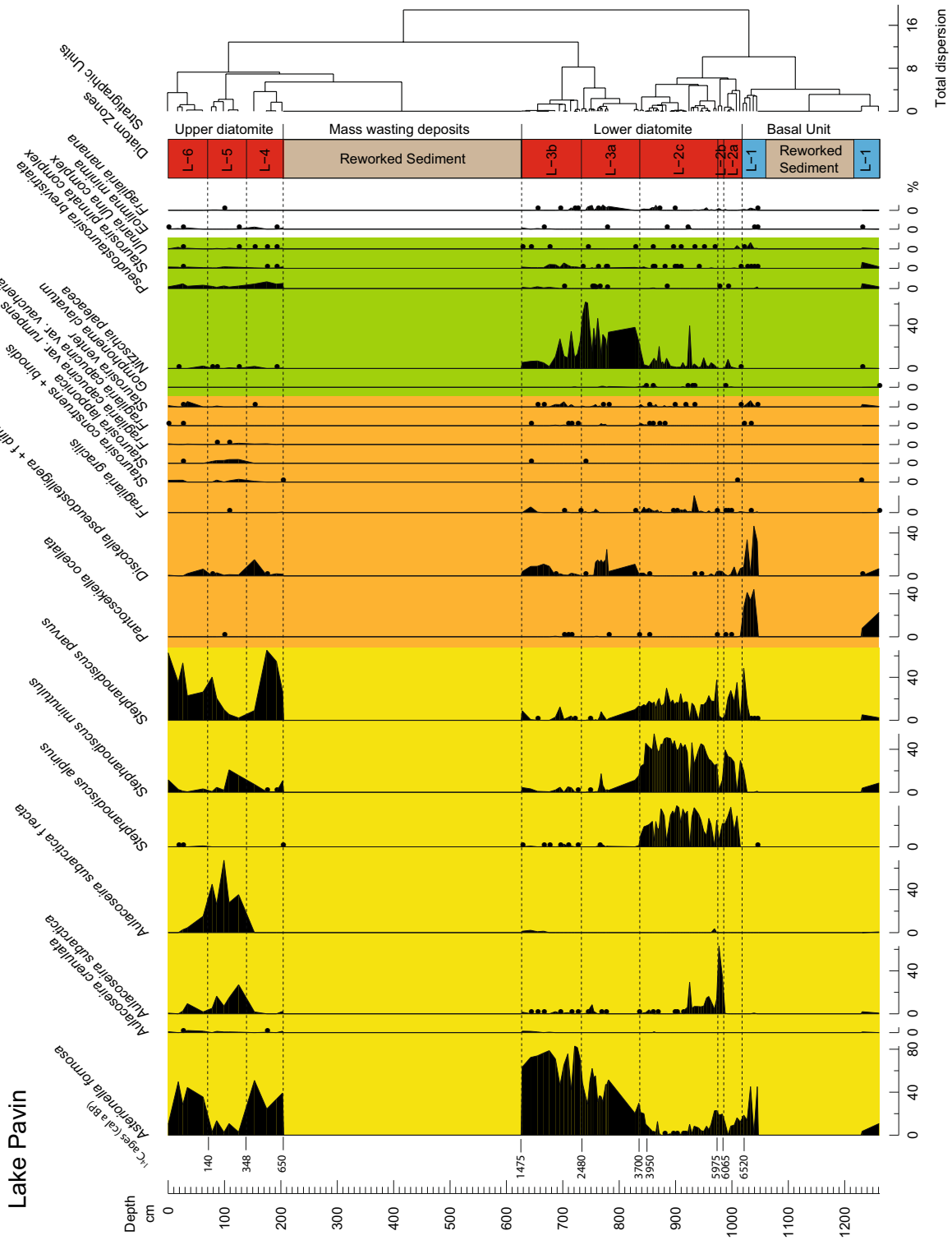
Lake Pavin
Depth cm
0
100
200
300
400
500
600
700
800
900
1000
1100
1200
140
348
650
1475
2480
3700
3950
5975
6065
6520
Upper diatomite
Mass wasting deposits
Lower diatomite
Basal Unit
L−6
L−5
L−4
Reworked Sediment
L−3b
L−3a
L−2c
L−2b
L−2a
L−1
Reworked Sediment
L−1
Total dispersion
0
8
16
Stratigraphic Units
Diatom Zones
Fragilaria nanana
Eolimna Una complex
Urosolenia Una complex
Staurosira brevistriata
Pseudostaurosira brevistriata
Nitzschia paleacea
Gomphonema clavatum
Staurosira venter var. rumpens
Staurosira capucina var. binodis
Fragilaria capucina
Fragilaria lapponica
Staurosira construens + binodis
Fragilaria gracilis
Discotella pseudostelligera + f dimmuta
Pantocsekiella ocellata
Stephanodiscus parvus
Stephanodiscus minutulus
Stephanodiscus alpinus
Aulacoseira subarctica f recta
Aulacoseira crenulata
Aulacoseira subarctica
Asterionella formosa
14C ages (cal a BP)
%
0
40
80

◂**Fig. 2** Diatom stratigraphic zonation based on 22 species was determined using CONISS with a content greater than 1% in more than one sample. Eight samples were missing between 828 cm and 778.5 cm. The stratigraphy is summarized as a lower basal unit (1400–1021 cm) composed of diatom-rich material interbedded with laminated volcanoclastic material and turbidites. The lower diatomite is between (1015–628 cm) with a mass wasting deposit (628–205 cm) between it and the upper diatom unit (203–0 cm). The euplanktonic species are marked in yellow, the tychoplanktonic in orange and the benthic–epontic species in Green. Red represents the diatomites, blue for the diatom layers in the basal unit, and brown the reworked layers

or alkaliphilous species that prefer more oxygen-saturated water with lower nutrient content. *Pantocsekiella ocellata* has a low Si requirement (Juggins 2001). *Discostella pseudostelligera*, a littoral, pelagic species (Houk et al. 2010, 2014), prefers low levels of nitrate, phosphates, and silica (Rioual 2000). Fragilarioid species (2–12%) have been associated with longer ice cover and colder winter conditions (Smol and Douglas 2007), but are also known to be some of the first taxa to develop in new forming lakes (Saulnier-Talbot and Pienitz 2001; Saulnier-Talbot et al. 2015). Other ecological indicators (Figs. 4 and 5) show that this zone had a high percentage of species that prefer waters with lower nitrogen content, lower pH and trophic state.

The lower unit, zone L-2 was divided into three subzones, L-2a (1015–988 cm; ca. 6490–6130 cal a BP), L-2b (983–977 cm; ca. 6070–5970 cal a BP) and L-2c, (973–838 cm; ca. 5910–3800 cal a BP). Major changes occurred in the lake, the trophic state of the waters along with pH and nitrogen increased while oxygen concentrations decreased. The *Stephanodiscus* species (*S. alpinus, S. minutulus and S. parvus*) are considered alkalibiontic (EDDI database, pH = 8.07). According to Rioual et al. (2007), *S. minutulus* implies long and deep vigorous spring circulation with low Si:P conditions under low but increasing light levels that suggest a dry winter that reduced the silicon loading in the lake. Kirilova et al. (2008) found similar results from sediment-trap study in Sacrower See (Germany). The increase in nutrients in the lake could have been caused by the continuous input of catchment-soil materials and volcanic products (both clastic and chemical). In zone L-2b, a small subzone (two samples studied), a pH change is noted with the circumneutral taxon *Aulacoseira subarctica*. According to Rioual et al. (2007), it also lives in circumneutral pH waters with low conductivity, low nitrate and high silica concentrations and low light conditions. While Cambrun and Charles (2000) found it in an aerated Clear Lake with a pH of 7.20 and TP of 4.5 µg L^{-1}. Gibson et al. (2003) found it with slight increase in eutrophication but, with continues increasing eutrophication it disappeared from the lakes. When TP concentrations fell below 30 µg L^{-1}, *A. subarctica* recovered. However, in the EDDI combined TP dataset (Juggins 2001), it has a TP optimum of 32.2 µg L^{-1}. *Aulacoseira subarctica* has a high sinking rate and occurs only in the water column when there is enough turbulence, often caused by windy conditions to keep it in suspension (Kilham et al. 1996). When thermal stratification develops, *A. subarctica* quickly sinks (Lund 1954). The periodic monitoring of Lake Pavin's mixolimnion has found an annual pattern of *D. pseudostelligera* and *S. parvus* developing in spring, and *A. subarctica* in autumn and winter. *Asterionella formosa* appears in spring and autumn, and *Cyclotella radiosa* in summer and autumn (not found in the sediments studied) (Devaux 1975; Rioual 2000; Rioual et al. 2007). The lake water becomes fresher with more saturation in oxygen, decrease in nitrogen and increase in oligotrophic to oligo-mesotrophic species. This could mark a short period of increased wind activity (or enhanced spring-freshwater supply) and induced currents during wet periods which would increase oxygen saturation, a decrease in nutrients, and the development of more oligotrophic and oligo-mesotrophic species. Both the upper two samples of zone L-1 and zone L-2 correspond to diversified forest with wooded area within the catchment and presence of heliophilous trees (PAV-1 pollen zone, Chassiot et al. 2018) (Figs. 4 and 5). Interestingly, the change from pollen zone PAV-1 to PAV-2 found at the end of diatom zone L-2b is marked by a peak of *A. subarctica* in the sediment. The gradual shift to nutrient-richer waters with lower oxygen concentration could be caused by slow development of soils in the developed catchment resulting from the phreatomagmatic explosion (Figs. 4 and 5).

The diatom zone L-2c, however, corresponds to two and half palynologic units (PAV-2, PAV-3 and PAV-4a, Figs. 4 and 5) identified by Chassiot et al. (2018). The lowest pollen zone, PAV-2 (977–933 cm,

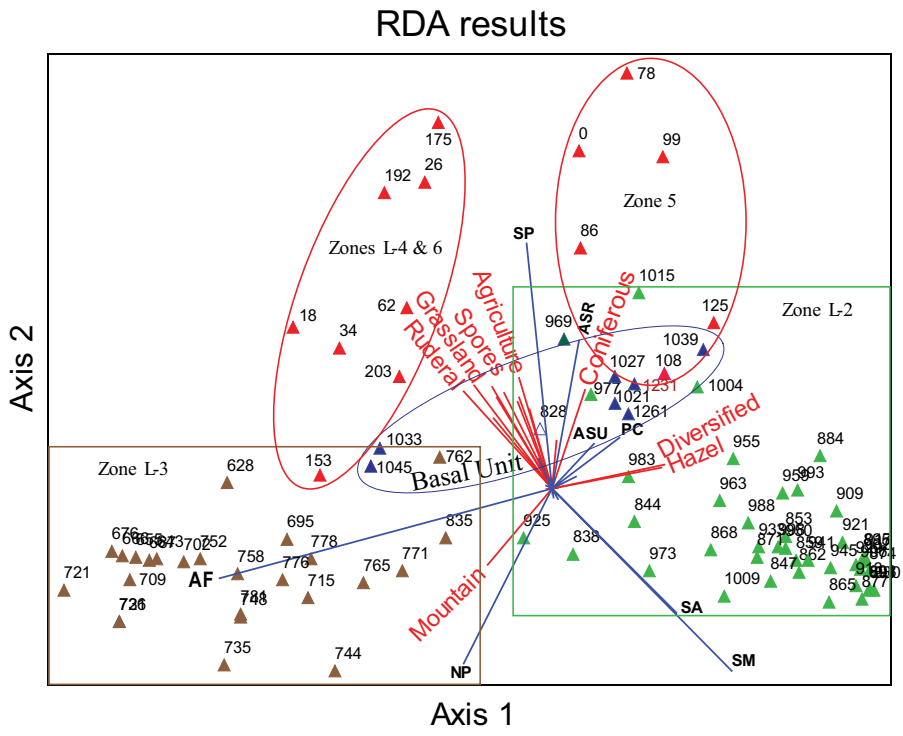

Fig. 3 Redundancy analysis of Lake Pavin samples based on species found in one or more samples with 5% or greater. AF = *Asterionella formosa,* ASR = *Aulacoseira subarctica* f. *recta,* ASU = *Aulacoseira subarctica,* NP = *Nitzschia paleacea,* PC = *Pantocsekiella ocellata,* SA = *Stephanodiscus alpinus,* SM = *Stephanodiscus minutulus,* and *Stephanodicus parvus* (SP). Basal unit zone L-1—blue full triangles, lower diatomite, zone L-2—green full triangles, zone L-3 brown full triangles, Upper diatomite, zones L-4, L-5, and L-6) red full triangles. Pollen factors: Apophytes = apophytes, Diversified = diversified oak woodland, Hazel = hazel, Mountain = mountain woodland, Coniferous = coniferous woodland, Agriculture = agriculture, Spores = spores, Grassland = grassland, and Ruderal = nitrophilous plus ruderal indicators and ruderals trampling indicators

ca. 5970–5220 cal a BP) saw the extension of the regional and local mountain woodland, while PAV-3 registered a moderate opening in the forest with the first record of Cerealia pollen, and PAV-4a (880–865 cm, ca. 5150–4470 cal a BP) marked the regular occurrence of Cerealia. Increased opening of the forest would enhance erosion and soil disturbance. The highest pH and trophic state (Fig. 5) are registered in this zone. The decrease and loss of *A. subarctica* would indicate an increase in lake eutrophication and an increase in *Stephanodiscus* taxa. Noted by Salmaso (2005) the complete circulation of lake waters would result in higher nutrient enrichment in comparison to circulation only in the epilimnion. During zone L-2, the Si curve shows the highest amounts of Si in the lake. The Si source comes from the catchment and the diatoms. One source of the Si is Si, enriched volcanic water that could be brought to the surface by complete mixing of the lake's waters.

The slow reduction in woodlands in L-2 may have reached a critical state where erosion increased, noted by an increase in fungi in the profile (Chassiot et al. 2018) and this could have caused a gradual downcutting of the outlet and increased inflow of sediment into Lake Pavin, marked an increase in TOC in L-3 (Fig. 5). As the water level in the lake decreases, areas lacking vegetation increase, permitting the increased inflow of sediment. During zone L-3, the euplanktonic diatoms (*Stephanodiscus* taxa) decrease from a maximum of 90% to less than 1% in certain samples and the tychoplanktonic-benthic diatoms increase from less than 1–50% in certain samples. Increase in sedimentary particles into the lake may have given the benthic diatoms more habitats to colonize, thereby causing a decrease in euplanktonic

diatoms as shown in Fig. 2. Taking into consideration the sedimentation rate in core PAV12 (Chassiot et al 2018) and available radiocarbon ages in soils (charcoal, peat or gytja materials) from trenches realized within and downstream of the Pavin crater, Thouret et al. (2021) determined that lake levels in Lake Pavin progressively dropped from 1214 m asl to 1206 m asl (i.e. 8 m) between 3950 and 3700 cal a BP. According to Wolin and Stone (2010), fewer planktonic species and an increase in periphytic community with a higher percentage of tychoplanktonic and benthic species indicate an increase in shallower areas, more clastic inwash, and a decrease in water depth.

Zone L-3 (835–628 cm; ca. 3760–1470 cal a BP) is composed of two subzones. *Nitzschia paleacea* increases in L-3a and decreases in L-3b, *Discotella pseudostelligera,* a eutrophic species (Van Dam et al. 1994; Denys 1991) reappears, while *Asterionella formosa* increases through L-3a and remains very high in L-3b. *Asterionella formosa* needs high Si, moderate to high P and N (Rioual et al. 2007; Hausmann and Pienitz 2009) and blooms in the spring (Voigt et al. 2008). According to Voigt et al. (2008), *N. paleacea* indicates higher concentration of NH_4 and has been associated with warmer water temperatures during the summer (Stoermer and Ladewski 1976; Rioual et al. 2007). There is also a marked increase in the total percentage of tychoplanktonic and benthic–epontic species (Fig. 2), which is usually taken to represent a phase of lower lake levels. There are several possibilities for periphyton increase: (1) the continuing lowering of lake levels could increase the periphytic zone with the possibility of more light reaching the plateau area within the crater. According to Jézéquel et al. (2016), the maximum limit of photosynthesis is 10–15 m depth for Lake Pavin. (2) An increase in the length of ice cover on the lake. In this case, it would give advantage to the periphytic species over the euplanktonic species, which develop later in the season. Note that the euplanktonic *Stephanodiscus* species are practically missing from this zone. *Nitzschia paleacea* was found in late summer and fall months in sediment traps in Sacrower See (Kirilova et al. 2008) while Bertrand et al. (2003) found a bimodal pattern for *A. formosa* occurring in winter-spring and autumn, which was also observed by others (Spaulding et al. 1993; Maberly et al. 1994). (3) Land-use changes within and around the crater could also affect conditions in the crater. A maximum development of *A. formosa,* a N-autotrophic diatom that requires elevated levels of nitrogen in diatom zone L-3b, supports this hypothesis. Diatom zone L-3a corresponds to pollen subzones PAV-4b and PAV-5a. PAV-4b saw the development of regional agriculture and clearance of breech woodland and woodland openings around the lake. Increased agricultural activities around the lake would mean increased runoff that would lead to increased erosion and more downcutting of the lake's outlet. A peak in the Ti curve occurs at the beginning of zone L-3a which supports increased input from the crater wall. Increased TOC input into the lake corresponds also to the beginning of zone L-3a. PAV-5a registered some renewal of woodlands with scattered open areas in the forest. Diatom zone L-3b is associated with pollen subzone PAV-5b that marked the regression of the woodland and some cereal cultivation near the maar. Ruderal and trampling indicators are also noted. A combination of cooler winters, decreasing lake levels and increased anthropogenic pressure seems to be the most likely explanations for these changes.

The change from *Stephanodiscus* taxa to *A. formosa* and *N. paleacea* marks chemical changes within the lake. Zone L-3 could signify the development of the meromictic situation that exists in the lake today. According to Salmaso (2005), complete overturn causes homogenization of the water column bringing up nutrient-rich water from the hypolimnion and mixing it with the epilimnion, but when incomplete overturn occurs, the epilimnion has lower concentrations in nutrients as less nutrient-rich waters including in the mixing. A decrease in trophic state and pH is observed in Fig. 5 for zone L-3 with axis 1 curve moving from negative scores to positive scores. However, under today's meromictic condition, an iron wheel has developed where Fe^{2+} is oxidized to aqueous Fe^{3+} in the transition zone between the mixolimnion and the monimolimnion (Busigny et al. 2016). The aqueous Fe_3^+ then reacts with other chemicals forming vivianite, pyrite or siderite which precipitates to the bottom of the lake. But, according to Chassiot et al. (2018), the iron wheel developed only with the formation of the upper diatomite where the Fe record is related to the oxidation and precipitation of Fe-rich porewaters in the upper unit. This was initially interpreted as an argument in favor of the development of the iron wheel in deep waters since the occurrence of MWDs. Nevertheless, the interpretation of redox

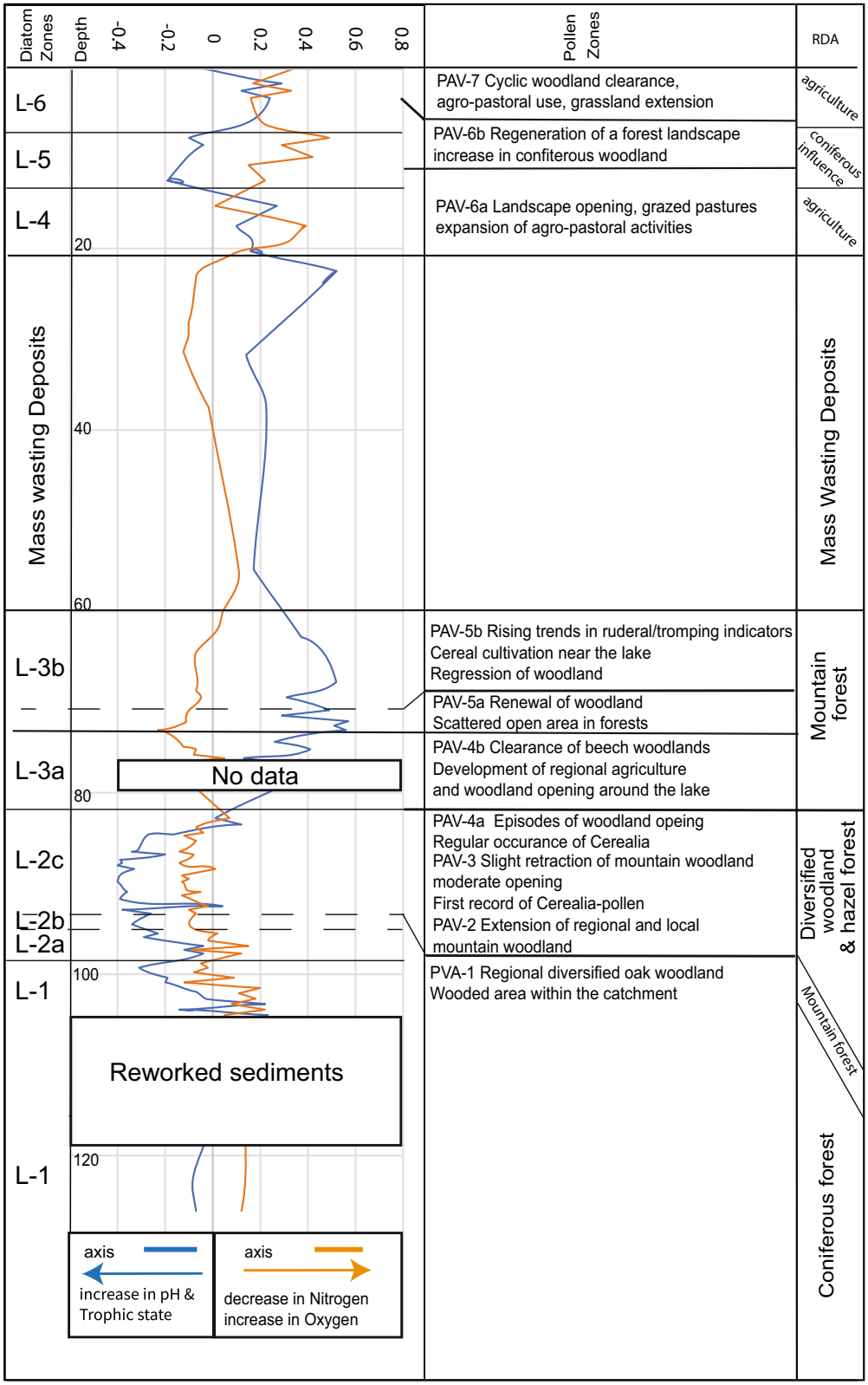
Diatom Zones
Depth
-0.4
-0.2
0
0.2
0.4
0.6
0.8
Pollen Zones
RDA
L-6
L-5
L-4
20
Mass wasting Deposits
40
60
L-3b
L-3a
80
No data
L-2c
L-2b
L-2a
100
L-1
Reworked sediments
120
L-1
axis
increase in pH &
Trophic state
axis
decrease in Nitrogen
increase in Oxygen
PAV-7 Cyclic woodland clearance,
agro-pastoral use, grassland extension
PAV-6b Regeneration of a forest landscape
increase in confiterous woodland
PAV-6a Landscape opening, grazed pastures
expansion of agro-pastoral activities
PAV-5b Rising trends in ruderal/tromping indicators
Cereal cultivation near the lake
Regression of woodland
PAV-5a Renewal of woodland
Scattered open area in forests
PAV-4b Clearance of beech woodlands
Development of regional agriculture
and woodland opening around the lake
PAV-4a Episodes of woodland opeing
Regular occurance of Cerealia
PAV-3 Slight retraction of mountain woodland
moderate opening
First record of Cerealia-pollen
PAV-2 Extension of regional and local
mountain woodland
PVA-1 Regional diversified oak woodland
Wooded area within the catchment
agriculture
coniferous influence
agriculture
Mass Wasting Deposits
Mountain forest
Diversified woodland & hazel forest
Mountain forest
Coniferous forest

◂**Fig. 4** Comparison of diatom RDA axis scores, pollen zones, and redundancy analysis. The gradual change from a conifer forest to diversified woodland with hazel, then to a mountain woodland and then to an agricultural dominated landscape with increase influence in diatom zone L-5 of conifer forest. The axes curves show the changes in water chemistry through time. Note the increase in conifer woodland in zone 5. This appears to be associated with the Little Ice Age

species profiles such as iron or manganese as proxies for anoxia are questionable, as they may reflect a modern redox front migrating into the sediment. Therefore, it is possible that the anoxia started earlier, and it would explain the major chemical change registered by the diatoms, but this is not supported by geochemical proxies in the lower unit (Fig. 5).

The upper unit is composed of three zones, zones L-4 (203–153 cm, ca. 650–400 cal a BP), L-5 (125–78 cm, ca. 290–160 cal a BP) and L-6 (62–1 cm, sub-recent). Our results correlate with the three zones (L-4 = DZ 1, L-5 = DZ 2, and L-6 = DZ 3) found by Stebich et al. (2005). Zone L-4 is dominated by *A. formosa* and *Stephanodiscus parvus*, both meso-eutrophic species. The peak in *S. parvus* corresponds with increased anthropogenic influences (Stebich et al. 2005) and this agrees with our results. *Stephanodiscus parvus* prefers nutrient-rich waters (Bennion 1994; Wunsam and Schmidt 1995). Fragilarioid species (*Pseudostaurosira brevistriata*, *Staurosira construens* complex, *Staurosirella lapponica*, *S. pinnata* complex) are always present throughout the three zones that may show an increasing influx

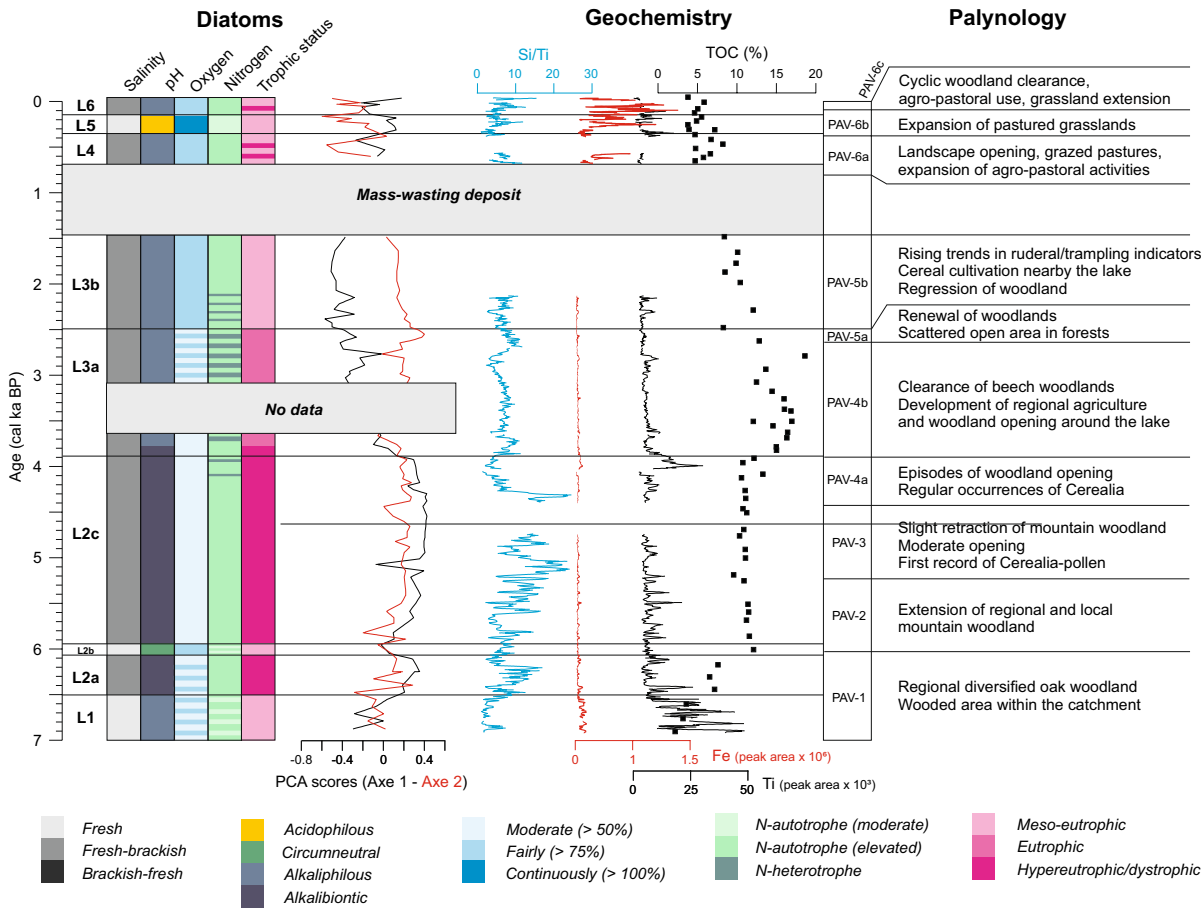

Fig. 5 Comparison of the diatom and pollen zones, PCA axis 1 and 2, and the following geochemical data—Si/Ti, Fe, Ti and TOC (Chassiot et al. 2016a, b). Axis 1 represents pH and trophic state, axis 2 nitrogen and oxygen (Fig. 4). Si maximum was registered for diatom zone L-2, while increase in Ti was noted for diatom zone L-3a

of sediment into the lake. The upper diatomite zones (L-4, 5 and 6) are similar to conditions observed in zone L-3. The trophic state decreases and oxygen content increases while pH decreases. This difference could be explained by incomplete overturn. In incomplete overturn, the hypolimnion would not be mixed with the epilimnion, thereby less nutrient enrichment. The landscape is opening with grazed pastures and expanded agro-pastoral activities (pollen zone PAV-6a).

In zone L-5 (290–160 cal a BP), *A. subarctica* and f. *recta* became the dominant species and fragilarioid species increased. *Aulacoseira subarctica* f. *recta* is considered a northern alpine species (Krammer & Lange-Bertalot 2000), prefers low water temperatures (Stoermer and Ladewski 1976; Rioual 2000; Rioual et al. 2007), and well adapted to low light conditions (Kilham et al. 1996). Its heavy frustule requires water circulation to remain in the water column (Kilham et al. 1986) as do fragilarioid species to put them in suspension. Fragilarioid taxa increase often during colder conditions. The increase in periphytic diatoms was also noted by Stebich et al. (2005) and could indicate longer autumn–winter conditions. Colder climatic conditions are also known to reduce the pH and here acidophilous diatoms increase. Increased acidity favors the liberation of more silica allowing for the development of the heavy *Aulacoseira* frustules. Epilimnion depth would also increase, bringing up more nutrient-rich waters from below (Salmaso 2005). The pH and trophic axis 1 curve (Fig. 5) shift to negative scores verifies increased nutient enrichment during this time. PAV-6b correlates to this diatom zone (Fig. 5), with reduced agro-pastoral activity and forest regeneration, and coniferous woodlands (Figs. 3 and 4). The above changes with extended ice cover could represent the Little Ice Age also suggested by Stebich et al. (2005).

Zone L-6 (62–1 cm, sub-recent) marks a return to similar condition as observed in L-4. PAV-7 registered cyclic woodland clearance with increased agro-pastural use of the uplands along with rye and hemp cultivation. With increased temperatures, the epilimnion shifts to oligomictic regimes with the continued mineralization in the hypolimnion that stabilizes the stratification (Lau et al. 2020), which is the situation observed today.

Conclusions

This multi-proxy research has provided a better comprehension of the evolution into the present-day regional mountain community and its relationship to changes observed within the lake. Anthropogenic influences have affected Lake Pavin from a relative very early date in its history. Combining diatom, pollen and geochemical data added to a possible explanation as to when meromixis developed. Diatoms showed several environmental changes that occurred over the 7000-years history. Major changes in diatom composition were related to changes in land use, development of meromixis, and geochemical and climate changes. The development of chemical-rich waters developed in zone L-2, dominated by *Stephanodiscus* species. The Si curve registered high input into the lake most likely coming from Si-rich volcanic waters into the lake. This corresponds to diversified woodlands. A major change in the diatom assemblage occurred between zones L-2 and L-3 and is related to increased forest openings and mountain woodlands. Incomplete overturn or meromixis developed. Si amount decreases and Ti has a peak at the beginning of this zone. Another diatom compositional shift was noted between zones L-4 and L-5 and is linked to climatic change and the depth of incomplete overturn, caused by the Little Ice Age. A shift from a strong agricultural influence in L-4 to an increased influence of coniferous woodland was noted. In zone L-6, there is a return to similar conditions as observed in zone L-4. Nevertheless, the strongest influence of agro-pastoral activities was registered in the upper diatomite.

Reported changes in Lake Pavin's limnology between 3950 and 3700 cal a BP give us an estimated date for the highest shoreline. A major shift from *Stephanodiscus* domination (zone L-2) to *Asterionella formosa, Discostella pseudostelligera* and *Nitzschia paleacea* assemblage (zone L-3) with decrease in planktonic species and increase in periphytic species occurred. This event is consecutive to a terrigenous input resulting from the erosion of a newly emerged littoral zone allowing more surfaces for periphytic species to be colonized. The joint action of human impact and/or climate deterioration would also favor erosion in the catchment during this period. The result was a progressive lake-level drop of ca. 8 m from 1214 m asl (earliest shoreline) to

1206 m asl (intermediate shoreline) and then a final drop of ~ 4 m to 1197 m asl. Stillstands 2 and 3 were not observed but may have occurred during the large MWD layer which lasted between 1475 and 650 cal a BP. The intermediate and lower terraces (Stages 2 and 3) identified on the lake shores are likely related to outlet incision and outburst flood events dated around AD 600 and AD 1280, respectively (Chassiot et al. 2016a; Chapron et al. 2021).

Acknowledgements Financial support came from CNRS INSU in the DICENTIM framework project, managed by Anne-Catherine Lehours. The French Region Centre give Léo Chassiot a PhD grant. The following laboratories should be thanked: EDYTEM (CNRS-University of Savoie-Mont Blanc, France) laboratory for the XRF core scanner analyses, the IRAMAT (CNRS-University of Orleans, France) laboratory for LA-ICP-MS analyses and the ARTEMIS program for radiocarbon dating. We would like to thank the reviewers for their very constructive criticism that led us to make a better article.

Author contributions Karen Serieyssol wrote most of the main text of the article. Emmanuel Chapron made Fig. 1, Karen Serieyssol made Figs. 2, 3 and 4, and Léo Chassiot made Fig. 5. Yannick Miras supplied the pollen database used in the DCA. Victor Arricau added new information about the ancient shoreline found within the crater. Karen Serieyssol compiled data in Table 1.

Declarations

Conflict of interest None of the authors have a conflict of interest with Springer Publishing.

References

AlgaeBase. World-wide electronic publication, National University of Ireland, Galway. https://www.algaebase.org

Arricau V (2020). Géohistoire des risques naturels de trois lacs de cratère emblématiques du Massif Central français (lacs Pavin, Tazenat et Issarlès). Master thesis University Toulouse Jean Jaurès, 104

Battarbee RW, Jones VJ, Flower BP, Cameron NG, Bennion H, Carvalho L, Juggins S (2001) Diatoms. In: Smol JP, Birks HJB, Last WM (eds) Tracking environmental change using lake sediments. Kluwer Academic Publishers, Dordrecht, pp 155–201

Beauger A, Voldoire O, Wetzel CE, Allain E, Millan F, Breton V, Kolovi S, Ector L (2020) Biodiversity and ecology of diatoms in mineral springs of the area of Sainte Marguerite (Saint-Maurice-ès-Allier, Massif Central, France). BIOM 1(1):21–37

Bennet KD (2002) Plotting and analysis program. Accessed July 2009, Available from: http://chrono.qub.ac.uk/psimpoll/psimcomb_manual/4.27/psman1.htm

Bennion H (1994) A diatom-phosphorous transfer function for shallow eutrophic ponds in southeast England. Hydrobiologia 275:391–410

Bertrand C, Fayolle S, Franquet S, Cazaubon A (2003) Response of the planktonic diatom *Asterionella formosa* Hassell to abiotic environmental factors in a reservoir complex (south-eastern France). Hydrobiologia 501:45–58

Bonhomme C, Jézéquel D, Poulin M, Saad M, Vinçon-Leite B, Tassin B (2016) Lake Pavin mixing: new insights from high resolution continuous measurements. In: Sime-Ngando T, Boivin P, Chapron E, Jézéquel D, Meybeck M (eds) Lac Pavin, Springer, AG Switzerland. https://doi.org/10.1007/987-39961-4_10

Busigny V, Jézéquel D, Cosmidis J, Viollier E, Benzerara K, Planavsky J, Albéric P, Lebeau O, Sarazin G, Michard G. (2016) The iron wheel in Lac Pavin: interaction with phosphorus cycle. In: Sime-Ngando T, Boivin P, Chapron E, Jézéquel D, Meybeck M (eds) Lac Pavin, Springer, AG Switzerland. https://doi.org/10.1007/978-3-319-39961-4_12.

Camburn KE, Charles DF (2000) Diatoms of Low-Alkalinity Lakes in the Northwestern United States. The Academy of Natural Sciences of Philadelphia, Pennsylvania, p 152

Chapron E, Albéric P, Jézéquel D, Wersteeg W, Bourdier J-L, Sitbon J (2010) Multidisciplinary characterisation of sedimentary processes in a recent maar lake (Lake Pavin, French Massif Central) and implication for natural hazards. Nat Hazards Earth Syst Sci 10:1–13

Chapron E, Foucher A, Chassiot L, Fleurdeus W, Arricau V, Perdereaux L, Gay-Ovejero I, Lavrieux M, Motellica-Heino M, Salvador-Blanes S (2021) Evaluating Holocene natural hazards in the French Massif Central from a regional lake sediment approach. Quat Int 636:134–153 https://doi.org/10.1016/J.quaint.2021.05.018

Chapron E, Ledoux G, Simonneau A, Albéric A, St-Onge G, Lajeunesse P, Boivin P, Desmet M (2012). New evidence of Holocene mass wasting events in recent volcanic lakes from the French Massif Central (lakes Pavin, Montcineyre and Chauvet) and implications for Natural Hazards. In: Yamada Y, Kawamura K, Ikehara K, Ogawa Y, Urgeles R, Mosher D, Chaytor J, Strasser M (eds.) *Submarine Mass Movements and Their Consequences*, Advances in Natural and Technological Hazards Research 31, Springer Science Business Media B.V. 2012, Chapter 23, 255–264

Chapron E, Chassiot L, Lajeunesse P, Ledoux G, Albéric P (2016) Lake Pavin sedimentary environments. In: Sime-Ngando T, Bouvin P, Chapron E, Jézéquel D, Meybeck M (eds) Lac Pavin, Springer, AG Switzerland. https://doi.org/10.1007/987-39961-4_22.

Chassiot L, Chapron E, De Giovanni C, Albéric P, Lajeunesse P, Lehours A-C, Meybeck M (2016b) Extreme events in the sedimentary record of maar Lake Pavin: implications for natural hazards assessment in the French Massif Central. Quat Sci Rev 141:9–25

Chassiot L, Miras Y, Chapron E, Develle A-L, Arnaud F, Motelica-Heino M, Di Giovanni C (2018) A 7000-year environmental history and soil erosion inferred from the deep sediments of Lake Pavin (Massif Central, France) Palaeogeogr Paleoclimatol Palaeoecol 497:218–233

Chassiot L, Chapron E, Miras Y, Schwab MJ, Albéri P, Beauger A, Déveille A-L, Arnaud F, Lajeunesse P, Zocatelli R, Bernard S, Lahours A-C, Ezéquel D (2016a). Lake Pavin paleolimnology and event stratigraphy. In: Sime-Ngando T, Boivin P, Chapron E, Jézéquel D, Meybeck M (eds) Lac Pavin, Springer, AG Switzerland, pp 381–406

Denys L (1991) A check-list of the diatoms in the Holocene deposits of the Western Belgian coastal plain with a survey of their apparent ecological requirements. I. Introduction, ecological code and complete list. Service Geologique de Belgique Professional Paper No 246. 41

Devaux J (1975) Dynamique des populations phytoplanctoniques dans deux lacs du Massif Central français. Annales De La Station Biologiques De Besse-En-Chandesse, Supplément 10:1–193

Gasse F (1969) Les sédiments à diatomées du Lac Pavin (Auvergne). Annales De La Station Biologique De Besse-En-Chandesse 4:221–237

Gibson CE, Anderson NJ, Haworth E (2003) Review *Aulacoseira subarctica*: taxonomy, physiology, ecology and palaeoecology. Eur J Phycol 39:83–101

Hall KJ, Northcote TG (2012) Meromictic Lakes. In: Herschy RW, Fairbridge RW, Bengtsson L (eds) Encyclopedia of Lakes and Reservoirs. Encyclopedia of Earth Sciences Series. Springer, Berlin

Harper M, McKay R (2010) Diatoms as markers of atmospheric transport. In: Smol JP, Stoermer EF (eds) The diatoms: applications for enivronmental and earth sciences. Cambridge University Press, Cambridge, pp 552–559

Hausmann S, Pienitz R (2009) Seasonal water chemistry and diatom changes in six beoral lakes of the Laurentian Mountains (Québec, Canada): impacts of climate and timber harvesting. Hydrobiologia 635:1–14

Hickel B, Håkansson H (1993) *Stephanodiscus alpinus* in Plußsee, Germany. Ecology, morphology and taxonomy in combination with initial cells. Diatom Res 8:89–98

Houk V, Klee R, Tanaka H (2010) Atlas of centric diatoms with brief key and description. Part III, Stephanodiscaceae A: *Cyclotella, Tertiarius, Discostella*. In Poulícková A (ed) Fottea 10 Supplement, 498

Houk V, Klee R, Tanaka H (2014) Atlas of centric diatoms with brief key and description. Part IV, Stephanodiscaceae B: *Stephanodiscus, Cyclostephanos, Pliocaenicus, Hemistephanos, Stephanocostis, Mesodictyon* & *Spicaticribra*. In Poulícková A (ed) Fottea 14 Supplement, 529

Jézéquel D, Sarazin G, Prévot F, Violier E, Groleau A, Agrinier P, Albéric P, Binet S, Bergonzini L, Micheard G (2011) Bilan hydrique de lac Pavin – water balance of the Lake Pavin. Rev Sci Nat d'Auvergne 74:75–96

Jézéquel D, Michard G, Viollier E, Agrinier P, Albéric P, Lopes F, Abril G, Bergonzini L (2016) Carbon cycle in the meromictic crater lake. In: Sime-Ngando T, Boivin P, Chapron E, Jézéquel D, Meybeck M (eds) Lac Pavin, Springer, AG Switzerland. https://doi.org/10.1007/987-319-39961-4_11

Juggins S (2001) The European Diatom Database. User guide (Version 1.2). 2001

Juvigné E, Miallier D (2016) Distribution, tephrostratigraphy and chronostratigraphy of the widespread eruptive products of Pavin volcano. In: Sime-Ngando T, Bovin P, Chapron E, Jézéquel D, Meybeck M (eds) Lac Pavin, Springer, AG Switzerland. https://doi.org/10.1007/987-319-39961-4_11

Kilham P, Kilham SS, Hecky RE (1986) Hypothesized resource relationship among African planktonic diatoms. Limnol Oceanogr 31:1169–1181

Kilham P, Theriot EC, Fritz SC (1996) Linking planktonic diatoms and climate change in the large lakes of the Yellowstone ecosystem using resource theory. Limnol Oceanogr 41:1052–1062

Kirilova EP, Bluszcz P, Heiri O, Cremer H, Ohlendorf C, Lotter AF, Zolitschka B (2008) Seasonal and interannual dynamics of diatom assemblages in Sacrower See (NE Germany): a sediment trap study. Hydrobiologia 614:159–170

Krammer K (2002) *Cymbella*. Diatoms Europe 3:584

Krammer K (2003) *Cymbopleura*, *Delicata*, *Navicymbula*, *Gomphocymbellopsis*, *Afrocymbella*. Diatoms of Europe 4:530

Krammer K, Lange-Bertalot H (1997a). Bacillariophyceae. 1. Teil: Naviculaceae. In: Ettl H, Gerloff J, Heynig H, Mollenhauer D (eds) Süsswasserflora von Mitteleuropa, 2(1), 876p

Krammer K, Lange-Bertalot H (1997b) Bacillariophyceae. 2. Teil: Bacillariaceae, Epithemiaceae, Surirellaceae. In: Ettl H, Gerloff J, Heynig H, Mollenhauer D (eds) Süsswasserflora von Mitteleuropa, 2(2), Gustav Fischer Verlag, Stuttgart, 611p

Krammer K, Lange-Bertalot H (2000) Bacillariophyceae. 3. Teil: Centrales, Fragilariaceae, Eunotiae. In: Ettl H, Gerloff J, Heynig H, Mollenhauer D (eds) Süsswasserflora von Mitteleuropa, 2 (3), Gustav Fischer Verlag, Stuttgart, 576p

Krammer K, Lange-Bertalot H (2004) Bacillariophyceae. 4. Teil: Achnanthaceae, kritische Ergänzungen zu *Navicula* (Lineoatae) und *Gomphonema*. In: Ettl H, Gärtner G, Heynig H, Mollenhauer D (eds) Süsswasserflora von Mitteleuropa, 2 (4), Spektrum Akademischer Verlag, Heidelberg, 468p

Kuehlthau-Serieyssol K (1993) Les diatomées des sédiments Lacustres d'âge Miocène supérieur d'Andance et Rochessauve (Ardèche). Paléoécologie, et Biostratigraphie. Thesis. Paris 6, Paris (France), 310

Lange-Bertalot H (2001) *Navicula* sensu stricto, 10 hreatomagmatic separated from *Navicula* sensu lato Frustulia. Diatoms Europe 2:526

Lau MP, Valero G, Pilotti M, Hupfer M (2020) Intermittent meromixis controls the trophic state of warming deep lakes. Sci Rep 10:12928. https://doi.org/10.1038/s41598-020-69721-5

Leyrit H, Zylber W, Lutz P, Jaillard A, Lavina P (2016) Characterization of phreatomagmatic deposits from the eruption of Pavin Maar (France). In: Sime-Ngando T, Bouvin P, Chapron E, Jézéquel D, Meybeck M (eds) Lac Pavin, Springer, AG Switzerland. https://doi.org/10.1007/987-39961-4_22

Lund JWG (1954) Further observations on the seasonal cycle of *Melosira italica* (Ehr.) Kütz. subsp *subarctica* O. Müll. J Ecol 43:151–179

Maberly SC, Hurley MA, Butterwick C, Corry JE, Heaney SI, Irish AE, Jaworski GHM, Lund JWG, Reynolds CS, Roscoe JV (1994) The rise and fall of *Asterionella formosa* in the south basin of Windermere: analysis of 45 -yr series of data. Freshw Biol 31:19–34

Manguin E (1954) Contribution à la connaissance biologique des boues lacustres du Lac Pavin (Puy-de-Dôme). Annales De L'ecole Nationale Des Eaux Et Forêts Et De La Station De Recherches Et Experiences 14(1):19

McCune B, Mefford MJ (2018) PC-ORD. Multivariate analysis of ecological data. Version 7.07. Wild Blueberry Media, Corvallis, Oregon, U.S.A.

Meybeck M (2016) Pavin, the birthplace of French limnology (1770–2012), and its degassing controversy (1986–2016). In: Sime-Ngando T, Boivin P, Chapron E, Jézéquel D, Meybeck M (eds) Lac Pavin, Springer, AG Switzerland. https://doi.org/10.1007/978-3-319-39961-4_1

Miallier D (2020) Variations récentes de niveau du lac Pavin: essai de mise en cohérence des différentes sources d'information BSGF. Earth Sci Bull 191:4

Olivier L (1952) Sur la présence en été dans le lac Pavin, d'une couche profonde dépourvue d'oxygène vers 70 m de profondeur. C R Académie Des Sci Paris (d) 234:743–745

Pailles C (1989) Diatoms from maar lake du Bouchet (Massif-Central, France): paleoenvironmental reconstruction since the last 120000 years (Les diatomées du lac de maar du Bouchet (Massif-Central, France): reconstruction du paléoenvironnement depuis les 120 derniers millénaires). Thesis. Aix-Marseille-2 Univ., 13 - Marseille (France), 283

Pastre J-F, Gauthier A, Nomade S, Orth P, Andrieu A, Goupille F, Guillou H, Kunesch S, Scaillet S, Randall RP (2007) The Alleret maar (Massif Central, France): a new lacustrine sequence of the early Middle Pleistocene in western Europe. C R Geosci 339(16):987–997. https://doi.org/10.1016/j.crte.2007.09.019

Pelletier J-P (1968) Un Lac méromictique, le Pavin (Auvergne). Annales De La Station Biologique De Besse-En-Chandesse 3:147–170

Pelletier J-P (1963) Température et oxygène dissous dans la couche profonde du lac Pavin. CR 88ème Congrès Sociétés Savantes, 2, 653–658

Rioual P (2002) Limnological characteristics of 25 lakes of the French Massif Central. Ann Limnol 38(4):311–327

Rioual P, Andrieu-Ponel V, de Beaulieu J-P, Reille M, Svobodova H, Battarbee RW (2007) Diatom response to limnological and climatic changes at Ribains Maar (French Massif Central) during the Eemian and Early Würm. Quat Sci Rev 26:1557–1609

Rioual P (2000) Diatom assemblages and water chemistry of lakes in the French Massif Central: a methodology for reconstruction of past limnological and climate fluctuations during the Eemian period. Unpublished Ph.D. thesis, University College London, London, 520p

Salmaso N (2005) Effects of climatic fluctuations and vertical mixing on the international trophic variability of Lake Garda, Italy. Limnol Oceanogr 50(2):553–565

Saulnier-Talbot E, Pienitz R (2001) Isolation au postglaciaire d'un bassin côtier près de Kuujjuaraapik-Whapmagoostui, en Hudsonie (Québec): une analyse biostratigraphie diatomifère. Géog Phys Quat 55:63–74

Saulnier-Talbot E, Larocque-Tobler I, Gregory-Eaves I, Pienitz R (2015) Response of lacustrine biota to Late Holocene climate and environmental conditions in northernmost Ungava (Canada). Arctic 68:153–168

Serieyssol K, Chatelard S, Cubizolle H (2010) Diatom fossils in mires: a protocol for extraction, preparation and analysis in palaeoenvironmental studies. Mires Peat 7:1–11

Sime-Ngando T, Boivin P, Chapron E, Jézéquel D, Meybeck M (2016) Lake Pavin. History, geology, biogeochemistry, and sedimentology of a deep meromictic maar lake. Springer, Berlin, p 421

Smol JP, Douglas MSD (2007) From controversy to consensus: making the case for recent climate change in the Arctic using lake sediments. Front Ecol Environ 5:466–474

Spaulding SA, Ward JV, Baron J (1993) Winter phytoplankton dynamics in a subalpine lake, Colorado U.S.A. Arch Hydrobiol 129:179–198

Stebich M, Brüchmann C, Kulbe T, Negendank JFW (2005) Vegetation history, human impact and climate change during the last 700 years recorded in annually laminated sediments of Lac Pavin, France. Rev Palaeobot Palynol 133:115–133

Stoermer EF, Ladewski TB (1976) Apparent optimal temperatures for the occurrence of some common phytoplankton species in southern Lake Michigan. Great Lake Res Div 18:1–49

Thouret J-C, Boivin P, Miallier D, Donnalieu F, Dummoulin JP, Labazuy P (2021) Post-eruption evolution of maar lakes and potential instability: the Lake Pavin case study, French Massif Central. Geomorphol 382:107663. https://doi.org/10.1016/j.geomorph.2021.107663

Van Dam H, Mertens A, Sinkeldam J (1994) A coded checklist and ecological indicator values of freshwater diatoms from the Netherlands. Aquat Ecol 28:117–133

Voigt R, Grüger E, Baier J, Meischner D (2008) Seasonal variability of Holocene climate: a palaeolimnological study on varved sediments in Lake Jues (Harz Mountains, Germany). J Paleolimnol 40:1021–1052

Wolin JA, Stone JR (2010) Diatoms as indicators of water-level change in freshwater lakes. In: Smol JP, Stoermer EF (eds) The diatoms: applications for the environmental and earth sciences. Second Edition, 174–185

Wunsam S, Schmidt R (1995) A diatom phosphorous transfer function for Alpine and pre-Alpine lakes. Mme Inst Ital Hydrobiol 53:85–99